

Viscoelastic response of sonic band-gap materials

I.E. Psarobas*

Department of Physics, National Technical University of Athens
Zografou Campus, GR-157 73, Athens, Greece

(Dated: December 2, 2024)

The effect of viscoelastic losses is introduced in a high density contrast sonic band-gap material of closed packed rubber spheres in air background. The scattering properties of such a structure are computed with an on-shell multiple scattering method in order to achieve results directly comparable to experiment. Direct comparison with the lossless case yields some very interesting features which are properly reported.

PACS numbers: 43.20.Fn; 43.40.Fz; 43.35.Cg; 43.35.Mr

The problem of wave propagation in inhomogeneous media is of great importance in many branches of physics, mathematics and engineering. In particular, matters such as the localization of classical waves¹ and the formation of spectral gaps in periodic elastic composites,^{2,3} seem to have drawn the attention of researchers over the last decade. Phononic or sonic crystals are composite materials which consist of homogeneous particles (solid or fluid inclusions the dimensions of which must be large enough in order for a macroscopic description of their elastic properties to be valid) distributed periodically in a host medium characterized by different mass density and Lamé coefficients. With an appropriate choice of the parameters involved one may obtain sonic crystals with absolute frequency gaps (omnidirectional sonic gaps).

Among the various method developed for the calculation of the elastic properties of phononic crystals, the traditional band-structure methods mainly deal with periodic, infinite, and nondissipative structures. However in an experiment, one fabricates finite-size slabs and the measurable quantities are, usually, the transmission and reflection coefficients. In addition, realistic structures do have losses, not to mention dispersion. This handicap was noticed in a theoretical study of colloidal crystals with ultrasound.⁴ A usual band-structure calculation proceeds with a given wave vector, \mathbf{k} , and computes the eigenfrequencies within a wide frequency range together with the corresponding eigenmodes. On the contrary, on-shell methods proceed differently, the frequency is fixed and one obtains the eigenmodes of the crystal for this frequency. Therefore, these methods are ideal when strongly dispersive materials are used for one, not to mention that in general on-shell methods are computationally more efficient than traditional band-structure methods.⁵ We have recently developed an on-shell method for phononic crystals,⁶ which applies to systems which consist of homogeneous spherical particles arranged periodically in a host medium characterized by different elastic coefficients. The method provides the complex band structure of the infinite phononic crystal associated with a given crystallographic plane; and also the transmission, reflection, and absorption coefficients of an elastic wave incident at any angle on a slab of the crystal, parallel to a given plane, of finite thickness.

The present work aims to introduce and discuss the effect of viscoelasticity in a sonic band-gap material. For this purpose, a binary system of close-packed rubber spheres in air is chosen. The viscoelastic response of the system is accounted by means of the Kelvin-Voigt model,⁷ which is well-suited for the materials and frequency regions of major interest. The problem of acoustic-wave scattering by a single viscoelastic sphere of radius S has been adequately addressed in the past⁷ according to the Kelvin-Voigt viscoelastic model. In such a case the sphere is considered to be elastic with modified shear and compressional complex wavenumbers, the imaginary parts of which represent a measure of the loss. In particular, for an absorbing sphere in an inviscid fluid background, the complex compressional and shear wavenumbers are conveniently defined as

$$q_{sl} = \frac{c_l}{c_{sl}} \frac{q_l}{\sqrt{1 - i[(\alpha + \beta)/\rho_s c_{sl}^2]}},$$

$$q_{st} = \frac{c_l}{c_{st}} \frac{q_l}{\sqrt{1 - i[\beta/\rho_s c_{st}^2]}}, \quad (1)$$

where $q_l = \omega/c_l$ refers to the fluid environment with ω being the angular frequency and c_l the respective speed of sound. The real parts of the complex Lamé parameters of the sphere, $\lambda_s = \lambda_{se} - i\lambda_{sv}$ and $\mu_s = \mu_{se} - i\mu_{sv}$, combined with the density ρ_s yield the compressional and shear wave speeds respectively

$$c_{sl} = \sqrt{(\lambda_{se} + 2\mu_{se})/\rho_s}, \quad c_{st} = \sqrt{\mu_{se}/\rho_s}. \quad (2)$$

The imaginary parts of the Lamé parameters are connected to the viscous losses $\alpha + 2\beta$, and β of the sphere as follows: $\alpha = \omega\lambda_{sv}$, $\beta = \omega\mu_{sv}$. The scattering problem of a solid sphere in an inviscid fluid⁸ is solved with the so-called scattering transition matrix, the elements of which, in the angular momentum representation (ℓ, m) (see Appendix), connect the spherical wave expansion coefficients⁶ of the scattered field in terms of the incident.

Multiple scattering effects of planes of spheres, sonic crystals and slabs of the same will enter this study via our newly developed method for phononic crystals.⁶ The reader may gain a fruitful insight going through the specifics of the above mentioned work. In brief, for the case of a sonic crystal, the method views it as a sequence

of planes of spheres parallel to a given surface: a crystallographic plane described by a two-dimensional (2D) lattice $\{\mathbf{R}_n\}$. The corresponding 2D reciprocal lattice we denote by $\{\mathbf{g}\}$. In the region between the n -th and the $(n+1)$ -th planes a Bloch wave solution for the displacement (harmonic time dependence is assumed) of the elastodynamic equation,⁸ corresponding to given frequency ω and a given reduced wave vector \mathbf{k}_{\parallel} within the surface Brillouin zone (SBZ) of the given surface, has the form

$$\mathbf{u}(\omega; \mathbf{k}_{\parallel}) = \sum_{\mathbf{g}} \{ \mathbf{u}_{\mathbf{g}n}^+ \exp[i \mathbf{K}_{\mathbf{g}l}^+ \cdot (\mathbf{r} - \mathbf{A}_n)] + \mathbf{u}_{\mathbf{g}n}^- \exp[i \mathbf{K}_{\mathbf{g}l}^- \cdot (\mathbf{r} - \mathbf{A}_n)] \}, \quad (3)$$

where

$$\mathbf{K}_{\mathbf{g}l}^{\pm} = (\mathbf{k}_{\parallel} + \mathbf{g}, \pm [(\omega/c_l)^2 - (\mathbf{k}_{\parallel} + \mathbf{g})^2]^{1/2}). \quad (4)$$

\mathbf{A}_n is a point between the n th and $(n+1)$ th planes. A generalized Bloch wave satisfies the equation

$$u_{\mathbf{g}n+1}^{\pm} = \exp(i \mathbf{k} \cdot \mathbf{a}_3) u_{\mathbf{g}n}^{\pm}, \quad (5)$$

where $\mathbf{a}_3 = \mathbf{A}_{n+1} - \mathbf{A}_n$ and $\mathbf{k} = (\mathbf{k}_{\parallel}, k_z(\omega; \mathbf{k}_{\parallel}))$. There are infinite many such solutions for given \mathbf{k}_{\parallel} and ω , corresponding to different values of the z -component, $k_z(\omega; \mathbf{k}_{\parallel})$, of the reduced wave vector \mathbf{k} , but in practice one needs to calculate only a finite number (a few tens at most) of these generalized Bloch waves. We have propagating waves [for these $k_z(\omega; \mathbf{k}_{\parallel})$ is real] which constitute the normal modes of the infinite crystal; and evanescent waves [for these $k_z(\omega; \mathbf{k}_{\parallel})$ is imaginary] which do not represent real waves, but they are mathematical entities which enter into the evaluation of the reflection and transmission coefficients of a wave, with the same ω and \mathbf{k}_{\parallel} , incident on a slab of the crystal parallel to the given surface. The transmission/reflection matrices for a slab which consists of a stack of layers of spheres with the same 2D periodicity parallel to a given plane of the crystal are obtained from the transmission/reflection matrices of the individual layers in the manner described in Ref. 6. Knowing the transmission/reflection matrices for the slab we can readily obtain the transmission, reflection, and absorption coefficients of a plane acoustic wave incident on the slab.

The system which will be examined here is a crystal of rubber spheres in air. The physical characteristics entering our calculations are taken from Ref. 7 and they definitely describe a realistic system. In particular, the mass density of air is $\rho_{air} = 1.2 \text{ kg/m}^3$ and its respective speed of sound $c_{air} = 334 \text{ m/s}$. The rubber spheres have a mass density $\rho_s = 1130 \text{ kg/m}^3$ and $c_{ts} = 1400 \text{ m/s}$, $c_{ls} = 94 \text{ m/s}$ compressional and shear speed of sound, respectively. In addition, three different viscoelastic levels are considered for the rubber spheres, namely: lossless spheres ($\alpha = \beta = 0$), a low viscous level ($\alpha_{low} = 0.5 \text{ MPa/s}$, $\beta_{low} = 0.01 \text{ MPa/s}$) and a high viscous level ($\alpha_{high} = 5 \text{ MPa/s}$, $\beta_{high} = 0.1 \text{ MPa/s}$).

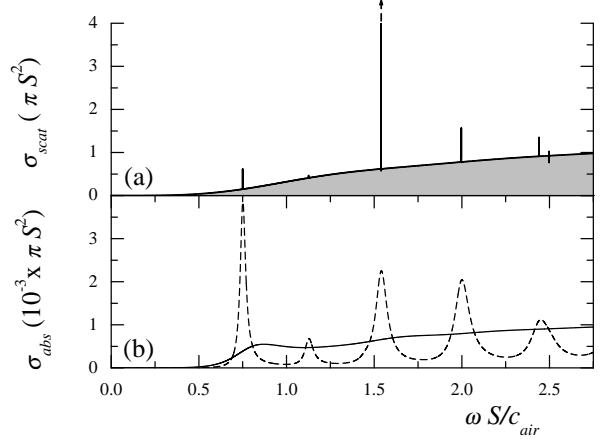


FIG. 1: (a): Normalized total scattering cross section of a rubber sphere in air. The solid line corresponds to a sphere with no losses and the shaded curve to a sphere with losses. The two different viscous levels used here, for the sphere, are hardly distinguishable. The resonance with the arrow extends twice as high. (b): Normalized absorption cross section of a viscoelastic rubber sphere. The dotted (solid) line corresponds to the low (high) viscous level used here.

Before embarking into the main object of this work, it will be of essence to repeat in brief certain basic features of the acoustic scattering problem by a viscoelastic sphere.⁷ These features will be used extensively in what is to follow. This brief outline is presented in Fig. 1, for an angular momentum cutoff, $\ell_{max} = 5$, which yields an accuracy of less than 0.001% in the given frequency range. On first sight, one can observe the disappearance of the sharp modal resonances in the scattering cross section of the sphere (see Appendix), when viscoelasticity is turned on. In addition, there is no significant difference between the two viscous levels (low and high) in scattering. On the contrary absorption (see Appendix) seems to exhibit different features for the two cases. The low viscous level induces resonant absorption exactly at the resonant frequencies of the lossless case, while the higher viscous level washes everything out as there was no inner resonant structure in the system.

We next consider an fcc crystal of close-packed rubber spheres in air background. We view the crystal as a succession of planes of spheres parallel to the (111) fcc surface. Fig. 2(a) shows the frequency band structure normal to the fcc (111) plane ($\mathbf{k}_{\parallel} = \mathbf{0}$) and the corresponding transmission spectrum for waves incident normally on a slab of the crystal consisting of 16 layers of lossless spheres. The results are obtained with an angular momentum cutoff $\ell_{max} = 7$ and 55 g vectors and the established convergence is within an accuracy of less than a tenth of a percent. At first sight one can observe, besides a large Bragg gap extending from $\omega S/c_{air} = 1.223$ to $\omega S/c_{air} = 2.065$, a considerable number of flat bands formed from the interacting sharp resonant modes of a single rubber sphere (see Fig. 1).

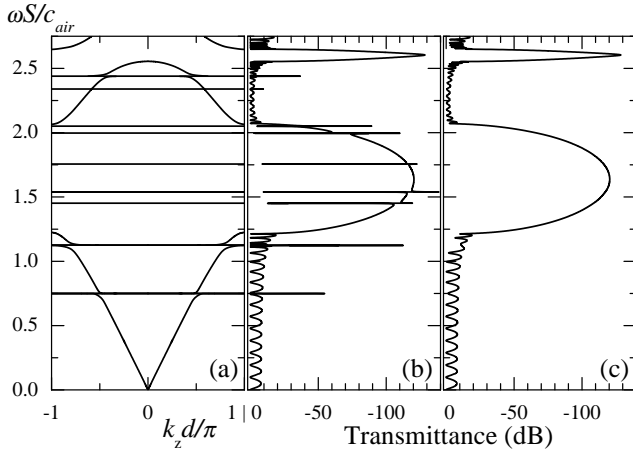


FIG. 2: The sonic band structure at the center of the SBZ of a (111) surface of an fcc crystal of closely packed lossless rubber spheres in air (a). The corresponding transmittance curve of a slab of 16 layers parallel to the same surface is given in (b). In (c) the same transmittance curve is presented but with spheres of the low viscous level. d is the distance between successive (111) planes of the fcc crystal under consideration.

These bands do have an inner structure as a consequence of the degeneracy removal of the appropriate contributing ℓ -modes in each case, due to interaction. We will not go any further on this since these bands are narrow in frequency, fact that makes them hardly observable. Their presence though, in the frequency spectrum, makes them noticeable by certain small hybridization gaps they induce above and below the main gap. This is clearly seen also in Fig. 2(b) in the transmission spectrum. Obviously inside region of the main gap these flat bands manifest themselves as sharp peaks in the transmission spectrum. The long wavelength limit is represented by the linear segments of the dispersion curves of Fig. 2(a), the slopes of which determine the propagation velocity of acoustic waves ($\bar{c}_l = 1.54 c_{air}$) in a corresponding effective medium. The oscillations in the transmission coefficient, over the allowed regions of frequency, are due to interference effects resulting from multiple reflection between the surfaces of the slab of the crystal (Fabry-Pérot-type oscillations). When losses are present in the system, there is no meaning dealing with the band structure of the “infinite” crystal, therefore the effect of the low viscous level is shown in the transmission spectrum [Fig. 2(c)]. As expected from the results of the single sphere, the sharp peaks and dips of the resonant states disappear and we obtain a “clean” sonic gap without any resonant modes within it. The existence of the frequency gap means that sound does not propagate through the crystal when its frequency lies within the gap (the intensity of the wave decays exponentially into the crystal for these frequencies), and if it cannot enter into the crystal, it cannot be absorbed either. This is shown in Fig. 3.

The close relation between absorption and transmission is demonstrated in Fig. 3 for slabs consisting of 8

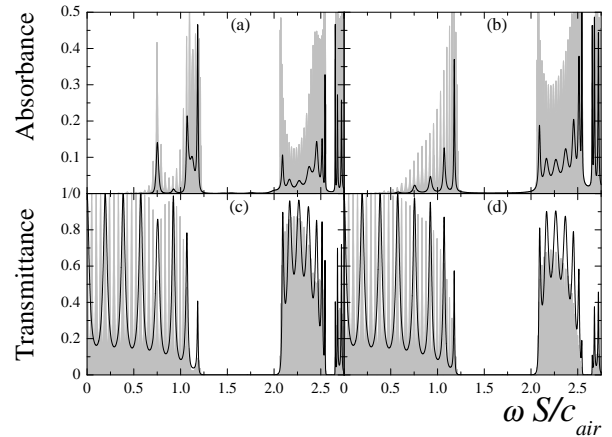


FIG. 3: Absorbance and transmittance curves of slabs of the rubber sonic crystal described in Fig. 2(a) consisting of 8 [(a),(c)] and 32 [(b),(d)] planes of spheres, respectively. The black line (shaded curve) corresponds to the low (high) viscous level.

and 32 layers of spheres, in the above mentioned (111) arrangement and at normal incidence. The solid lines correspond to the lower viscous level and the shaded curves to the higher one. A relatively large transmission coefficient implies that a relatively large fraction of sound has gone through the slab, which implies a correspondingly high probability of being absorbed. It is also evident that absorption is strong at the vicinity of the gap edges and decays rapidly away from them, fact which is emphasized with an increasing thickness of the slab. These observations are strongly supported by the case with the high viscous level, since they closely follow the Fabry-Pérot oscillations of the transmitted field. The absorption pattern of the low viscous level follows more or less the resonant modes associated with the single sphere resonances independently of the thickness of the slab. Expected quantitative results for the high and low viscous levels are observed and in conjunction with the thickness of the slabs.

In Fig. 4 the projection of the frequency band structure on the SBZ of the (111) plane of the fcc crystal along its symmetry lines is shown. This is obtained, for a given \mathbf{k}_{\parallel} , as follows: the regions of frequency over which there are no propagating states in the “infinite” crystal [the corresponding values of all $k_z(\omega, \mathbf{k}_{\parallel})$ are complex] are shown in white, against the shaded areas which correspond to regions over which propagating states do exist [for a given ω there is at least one solution corresponding to $k_z(\omega, \mathbf{k}_{\parallel})$ real]. One clearly sees here how the interacting sharp resonances of sphere appear forming narrow hybridization gaps above and below the main gap and flat bands in the gap regions. The crystal under investigation here exhibits, when losses are present, an appreciable omnidirectional sonic gap extending from $\omega S/c_{air} = 1.595$ up to 1.946. This absolute frequency gap has a width over midgap frequency of 20%, a rare property for sonic crys-

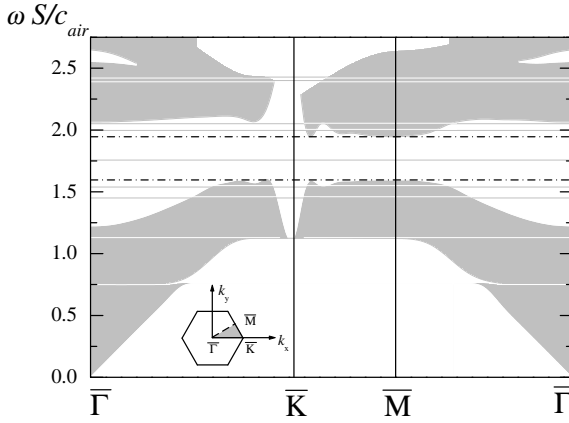


FIG. 4: Projection of the frequency band structure on the SBZ of the (111) surface of the fcc sonic crystal described in the caption of Fig. 2(a). The white areas show the frequency gaps in the considered frequency region. The broken lines map the absolute frequency gap of the system with losses. Finally, the inset shows the SBZ of the (111) surface.

tals with continuous network topology.⁹ It is suspected that this is due to the enormous density contrast between rubber and air. Finally, we may add that this gap is robust regardless of the amount of losses that are present in the system, for reasons explained in detail above.

A high density contrast sonic crystal of closely packed viscoelastic rubber spheres in air was examined here and the results of this investigation demonstrated the existence of an appreciable omnidirectional sonic gap. The robustness of the gap under losses may give rise to possible applications in different domains of frequency ranges since the results scale with the size of the spheres. This is true, provided that the viscoelasticity model used here is appropriate in the frequency range of preference for the description of the acoustic and in general the elastic field. The present study provides the means of a more realistic description of such sonic band-gap materials in order to achieve a closer connection of theory with experiment.

Acknowledgments

This work has been supported by the Institute of Communication and Computer Systems (ICCS) of the National Technical University of Athens. Support from the University of Athens is also acknowledged.

APPENDIX A

Applying the proper boundary conditions at the interface between the surrounding fluid and the sphere,⁸ re-

quiring the continuity of the radial component of the displacement field and the surface traction, along with the requirement that there is no tangential component of the surface traction at the interface, we can very easily determine the scattering matrix which connects the incident with the scattered field. Here for reasons of completeness, along the lines of formalism established in Ref. 6, the nonzero elements of the \mathbf{T} matrix for a solid sphere in a fluid host are

$$T_{\ell m; \ell' m'}^{LL} = \frac{W_{\ell}^{LL}}{D_{\ell}} \delta_{\ell \ell'} \delta_{m m'} , \quad \ell, \ell' \geq 0 , \quad (A1)$$

with $z_l = S q_l$ referring to the fluid and $x_{\nu} = S q_{s\nu}$ with $\nu = l, t$ to the sphere. The superscripts LL refer to the case of scattering for a fluid host, since incident and scattered waves are L -type compressional waves. The 3×3 determinants D_{ℓ} and W_{ℓ}^{LL} are given by

$$D_{\ell} = \begin{vmatrix} d_{22} & d_{23} & d_{24} \\ d_{32} & d_{33} & d_{34} \\ d_{42} & d_{43} & d_{44} \end{vmatrix} , \quad W_{\ell}^{LL} = - \begin{vmatrix} d_2^L & d_{23} & d_{24} \\ d_3^L & d_{33} & d_{34} \\ d_4^L & d_{43} & d_{44} \end{vmatrix} , \quad (A2)$$

where

$$\begin{aligned} d_{22} &= z_l h_{\ell}^{+'}(z_l), \quad d_{23} = \ell(\ell+1) j_{\ell}(x_t), \\ d_{24} &= x_l j_{\ell}'(x_l), \quad d_{32} = 0, \\ d_{33} &= [\ell(\ell+1) - 1 - x_t^2/2] j_{\ell}(x_t) - x_t j_{\ell}'(x_t), \\ d_{34} &= x_l j_{\ell}'(x_l) - j_{\ell}(x_l), \quad d_{42} = -x_t^2 \rho h_{\ell}^{+}(z_l)/(2\rho_s), \\ d_{43} &= \ell(\ell+1) [x_t j_{\ell}'(x_t) - j_{\ell}(x_t)], \\ d_{44} &= [\ell(\ell+1) - x_t^2/2] j_{\ell}(x_l) - 2x_l j_{\ell}'(x_l), \\ d_2^L &= z_l j_{\ell}'(z_l), \quad d_3^L = 0, \quad d_4^L = -x_t^2 \rho j_{\ell}(z_l)/(2\rho_s). \end{aligned} \quad (A3)$$

j_{ℓ}' and h_{ℓ}^{+} denote the first derivatives of the spherical Bessel and Hankel functions, respectively. The \mathbf{T} matrix, because of spherical symmetry is diagonal in ℓ and independent of m . The exact form of the above \mathbf{T} matrix allow us to compute the normalized total scattering cross section of an elastic sphere in a fluid host

$$\sigma_{total} = \frac{4}{z_l^2} \sum_{\ell=0} (2\ell+1) |T_{\ell m; \ell m}^{LL}|^2 , \quad (A4)$$

where $z_l = S q_l$ and S is the radius of the sphere. In addition the normalized absorption cross section is given by

$$\sigma_{abs} = - \frac{4}{z_l^2} \sum_{\ell=0} (2\ell+1) \left\{ |T_{\ell m; \ell m}^{LL}|^2 + \text{Re}[T_{\ell m; \ell m}^{LL}] \right\} . \quad (A5)$$

* Also at the Section of Solid State Physics of the University of Athens, Panepistimioupolis, GR-157 84, Athens, Greece.;

uoa.gr/~vyannop

- ¹ *Scattering and Localization of Classical Waves in Random Media*, edited by P. Sheng (World Scientific, Singapore, 1990); P. Sheng, *Introduction to Wave Scattering, Localization and Mesoscopic Phenomena* (Academic Press, San Diego, 1995).
- ² M. M. Sigalas, and E. N. Economou, *J. Sound Vib.* **158**, 377 (1992).
- ³ M. S. Kushwaha, P. Halevi, L. Dobrzynski, and B. Djafari-Rouhani, *Phys. Rev. Lett.* **71**, 2022 (1993).
- ⁴ R. Sprik and G.H. Wegdam, *Solid State Commun.* **106**, 77 (1998).
- ⁵ Y. Qiu, K.M. Leung, L. Carin, and D. Kralj, *J. Appl. Phys.* **77**, 3631 (1995).
- ⁶ I. E. Psarobas, N. Stefanou, and A. Modinos, *Phys. Rev. B* **62**, 278 (2000).
- ⁷ V. M. Ayres and G. C. Gaunaurd, *J. Acoust. Soc. Am.* **81**, 301 (1987).
- ⁸ D. Brill and G. Gaunard, *J. Acoust. Soc. Am.* **81**, 1 (1987).
- ⁹ E.N. Economou and M.M. Sigalas, *Phys. Rev. B* **48**, 13434 (1993).